

Mathematical Modeling of Triglyceride Transesterification through Enzymatic Catalysis in a Continuous Flow Bioreactor

A. V. Borgolov, K. V. Gorin*, V. M. Pozhidaev, Y. E. Sergeeva, P. M. Gotovtsev and R. G. Vasilov

National Research Center «Kurchatov Institute», Moscow, Russia; borgoloff@gmail.com, gkvbio@gmail.com, pojidaev2006@yandex.ru, yanaes2005@gmail.com, gotovtsevpm@gmail.com, raifvasilov@mail.ru

Abstract

Background: Currently, the production of biodiesel in many countries is a rapidly developing industrial sector. This article reviews the mathematical modeling of the enzyme-catalyzed triglyceride transesterification, which takes place in a continuous flow bioreactor. **Findings:** A mathematical model was developed and used to calculate the transesterification of microalgae lipids. The model developed was tested by conducting a laboratory experiment for similar conditions. It was shown that the difference between the data obtained according to the simulation results using a mathematical model and the experimental data was less than 5%. **Improvements:** The materials of the article are of practical value because the developed mathematical models can be used at the stage of manufacturing engineering or when designing new continuous flow bioreactors. These models can be useful when creating new types of catalyst loading for the existing bioreactors.

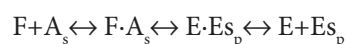
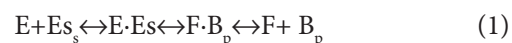
Keywords: Biodiesel Fuel, Enzymes, Enzyme Catalysis, Enzyme Immobilization, Genetic Modifications, Immobilization of Cells, Immobilization of Yeast Cells, Mathematical Modeling, Yeast

1. Introduction

Currently, the production of biodiesel is a rapidly developing industrial sector in many countries. An interest in biodiesel is caused by both the environmental concerns and the considerations of energy independence. The most common method of biodiesel production is the transesterification of triglycerides to obtain fatty acid esters¹. This is a catalytic process. Various solid catalysts, such as ferrous sulfate or metal-oxide systems, can be found among the catalysts used. In addition, serious consideration is paid to the use of enzymes (lipases) as catalysts. At present, it is shown that enzymatic catalysis has a number of advantages including the low thermodynamic parameters of the process, the glycerol of better quality, which can be used in industry, etc.^{1,2} However, the mathematical models of the biodiesel production process have been currently

developed, which are implemented at the laboratory level in flasks and bioreactors with mechanical agitation³. At the same time, a promising solution is to use the continuous flow bioreactors, which have a lower metal content and allow the creation of more compact productions with the same product throughput⁴.

The transesterification reaction can generally be written as follows¹:



where: A_s is the alcohol used in the process;

B_p is the process product (di-, monoglyceride or glycerin);

E is a free enzyme (lipase);

E_s is an original process substance (tri-, di- or monoglyceride);

*Author for correspondence

Es_p are the fatty acid esters;

F are the fatty acids.

The same as many enzyme-involving processes discussed in this article, the process of producing biodiesel fuel can be described by using the Michaelis–Menten kinetics. The result of this description is represented in the following equation (2)^{1,2}:

$$v_j = \frac{V_{max}(1 - e^{-k_d})[jG][A]}{K_{m,j}[A](1 + [A]/K_{i,A}) + K_{m,A}[jG] + [jG][A]} \quad (2)$$

$$\times \left(1 - \frac{[B_P][Es_P]/[jG][A]}{K_{eq,j}}\right)$$

where: v_j is the initial velocity of the process;

$K_{m,j}$, $K_{m,A}$ are the kinetic constants, j is for mono-, di- and triglycerides, A is for a substance that is an acyl group acceptor;

$[jG]$ is a concentration of mono-, di- and triglycerides (in accordance with the j number);

k_d is a constant of the process deactivation in accordance with the Arrhenius equation;

$K_{eq,j}$ is an equilibrium constant for the process involving the j -th substance.

The reaction scheme is as follows: the ester hydrolysis step is followed by the esterification step, which forms a new ether linkage by interaction between the released free fatty acids and the incoming alcohol group. Figure 1 shows the main steps of esterification and hydrolysis reaction with a catalyzing enzyme (lipase) (E) interacting with a triglyceride (T). First, the enzyme forms a first complex (E · T), and T is then hydrolyzed to a diglyceride (D) and a

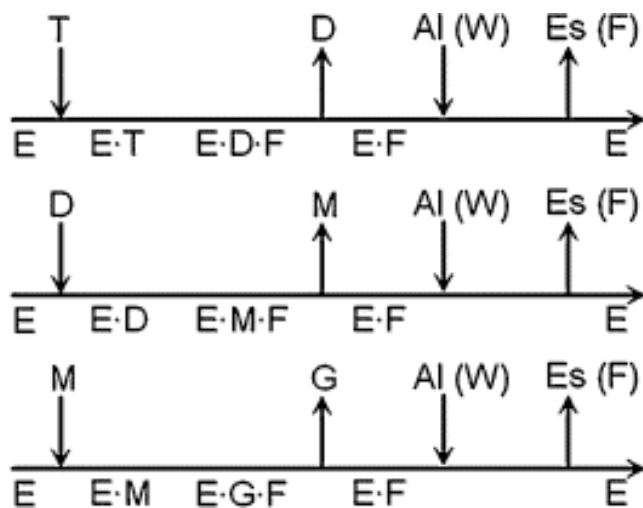


Figure 1. The scheme of the triglycerides enzymatic hydrolysis reaction.

fatty acid (F). Subsequently, D is released from the second complex (E · D · F) to form the third complex (E · F). This complex can be reactive with an alcohol (Al) through an alcoholysis reaction to form alkyl ester (ES) or with water (W) through a hydrolysis reaction to release F enzyme. Accordingly, the diglyceride (D) and the monoglyceride (M) hydrolysis mechanisms are similar to the enzymatic triglyceride hydrolysis described above. It should be noted that the nature of interaction between the alcohol molecules and the active site of lipase can strongly depend on both the lipase-carrying microorganism and the physico-chemical properties of the system as a whole (chemical composition of fats, temperature, pH, lipase immobilizing method, etc.)⁵.

In order to develop a mathematical model of the process of biodiesel fuel production using a mixer with mechanical agitation, several kinetic models obtained by adapting the results of the study⁶ on the reaction mechanisms of an enzyme catalysis involving ethanol and methanol were investigated for the purposes of this study.

The main features of kinetic models involve various limiting stages and different points of methanol molecules entry into the catalytic cycle. However, all the mechanisms underlying these kinetic models are based on three general assumptions:

- since the preliminary experimental results show that the reaction rate is slow enough, the possible skin effects on the surface of enzyme carriers (for example, adsorption of fats on the cell walls) can be neglected. This assumption is based on the analysis of experimental data on the kinetics of the studied reactions performed earlier³ as well as on the analysis of the data published in the literature^{7,8};
- all fatty acids produced during the reaction can be considered as a single reaction component (F) (that is, the differences between them are not taken into account);
- inhibition of the enzyme activity with alcohol should be considered as a competitive mechanism of inhibition.

When developing a mathematical model for a mechanically agitated mixer, the four kinetic models currently available in the scientific literature (hereinafter referred to as the kinetic models 1–4) were considered. The parameters of kinetic models were determined on the basis of experimental data on the basic steps of esterification

hydrolysis reaction being part of a complete kinetic cycle of the reaction shown in Figure 2^{2,8}. These models will be briefly discussed hereinafter.

By using the mechanism of kinetic model 1 based on the generalized reaction scheme shown in Figure 2, you can get a number of expressions for reaction yield for various cases through varying the intermediate stages that limit the overall rate of reaction. Indeed, the transesterification reaction scheme under consideration includes sequential execution of the intermediate hydrolysis and esterification reactions and thus requires multiple points for the reactant injection and the product removal so that to match the overall reaction mechanism. Furthermore, the activity of some lipases is limited by the kinetics of an intermediate reaction destructing the enzyme-substrate complex⁶. Thus, the kinetic model 1 involves the expressions for the formation rates of hydrolysis and synthesized fatty acid methyl ester intermediates, in which the intermediate reactions are limiting. At the same time, the other intermediate reactions are expected to establish a rapid equilibrium.

The mechanism of kinetic model 2 (Figure 3) differs from the mechanism of kinetic model 1 in the stages that are responsible for the destruction of the

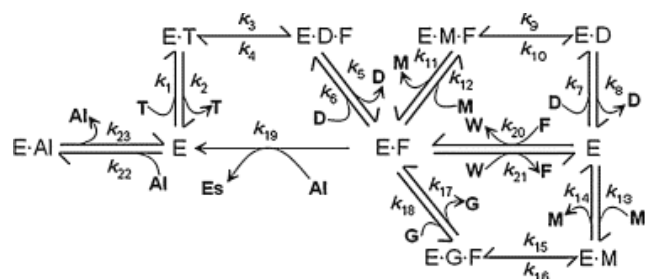


Figure 2. The general scheme of the reaction mechanism in the kinetic model 1, k_i is a constant of the corresponding reaction.

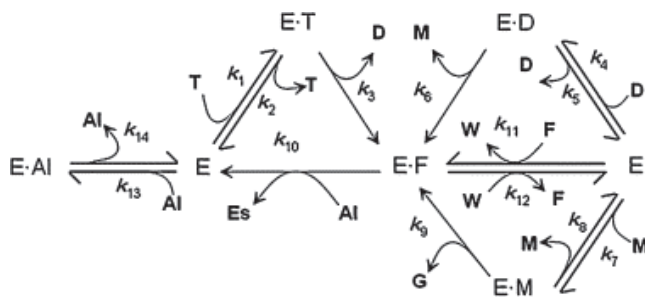


Figure 3. The general scheme of the reaction mechanism in the kinetic model 2.

enzyme-intermediate complexes after the hydrolysis reaction. Accordingly, to simplify this mechanism, an assumption is used concerning the rapid destruction of the complex involving an enzyme with the intermediate reaction products after the hydrolysis step. This assumption is based on an analysis of a variety of published data on the kinetics of the catalytic reaction mechanisms with the use of lipases³. Accordingly, the expressions for the intermediates production rates may be simplified in this model.

The kinetic model 3 differs conceptually from the kinetic models 1 and 2 in the stages that include reaction with an alcohol. Indeed, several studies have shown that the transesterification reaction can proceed according to the mechanism of a direct triglyceride alcoholysis instead of the two-stage mechanism comprising the successively proceeding stages of hydrolysis and esterification⁵⁻⁶. Thus, the kinetic model 3 has a general scheme for the enzymatic catalysis reaction represented by two groups of reactions. The first group represents the two-stage reactions, in which the hydrolysis step occurs prior to the esterification step. The second group represents the reactions of direct alcoholysis, which immediately form the fatty acid methyl esters. In practice, both types of these reactions can take place simultaneously. Thus, the reaction scheme used in the kinetic model 3 consists of a series of parallel reactions for each of the complexes considered ($E \cdot T$, $E \cdot D$ and $E \cdot M$). The general reaction mechanism scheme of the kinetic model 3 is shown in Figure 4.

An analysis of the published study results concerning the kinetics of the catalytic transesterification reactions involving the immobilized lipase and alcohol has shown that the kinetic model 3 best reflects the transesterification

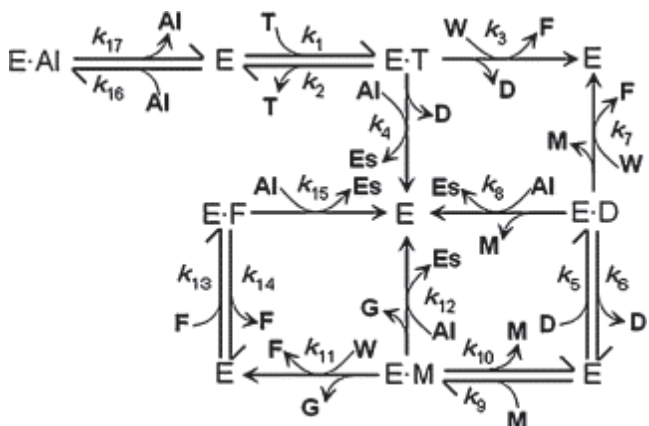


Figure 4. The general scheme of the reaction mechanism in the kinetic model 3.

process⁵. However, despite the above mentioned, the kinetic model 3 has a significant drawback—it does not describe the increasing concentration of water within the esterification. As shown in several studies^{5,9}, the water concentration during the transesterification reactions involving lipases varies with time due to the accumulation of water liberated during the reaction of fatty acids with the alcohol molecules.

Since water plays an important role in a variety of physical and chemical processes occurring in the reactor (the separation of the hydrophilic and hydrophobic phases, the kinetics of concurrent processes, etc.), this effect is taken into account when developing a mathematical model for the process of biodiesel fuel production.

By using the results presented in the study⁹, the kinetic model 3 was improved through introducing small changes into the overall scheme of the transesterification reaction so that the changed kinetic model can quantitatively describe the accumulation of water during the transesterification reaction. This kinetic model (model 4) is shown in Figure 5. In accordance with this scheme, E reacts with Al, T, D, M, and F) to form the bonded complexes: $E \cdot Al$, $E \cdot T$, $E \cdot D$, $E \cdot M$, and $E \cdot F$. Thus, this model involves simultaneous reaction of hydrolysis and esterification, wherein the $E \cdot T$, $E \cdot D$, and $E \cdot M$ complexes can react with W, forming fatty acids, or with A, forming Es, which ultimately leads to the formation of glycerin (G).

Thus, it can be concluded that today there is enough data to develop the mathematical models of the process of biodiesel production for the various types of bioreactors. The aim of this study is to develop a mathematical model

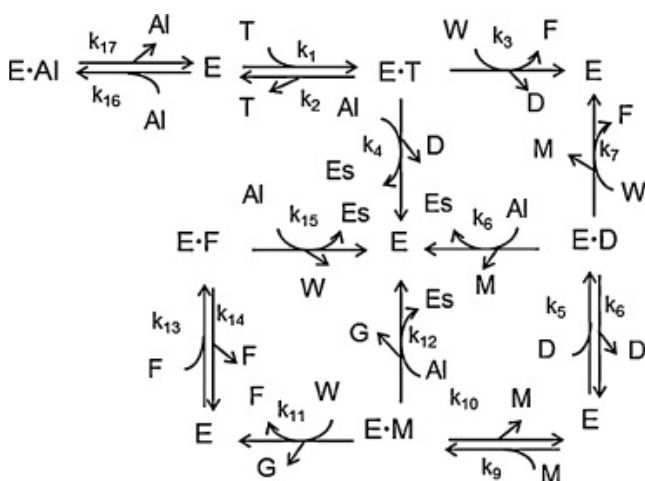


Figure 5. The general scheme of the reaction mechanism in the kinetic model 4.

for the continuous flow bioreactor and its validation on the experimental data.

2. Materials and Methods

2.1 Mathematical Model Description

The mixture of oil and alcohol in the production of biodiesel fuel is a two-phase system in the form of an emulsion with various oil/alcohol ratios. For now, the motion of the two-phase flows through the granular bulk units has been poorly understood. In addition, the mathematical description of the two-phase flow motion encounters great difficulties due to the extreme complexity of the structure of these flows. The difficulty lies in the fact that the disperse phase is usually unevenly distributed across the flow section and its local concentrations typically vary along the flow length, wherein both phases are moving at different speeds influencing each other. When pumping the emulsion consisting of oil and alcohol, the joint adsorption of alcohol and oil molecules occurs in a downward direction on the surface of grains through the granular catalyst device. Moreover, a less viscous fluid clogs the pores and ultimately reduces the total flow rate. The Flow pattern is further complicated in cases where the dispersed phase consists of particles with different sizes and densities.

There are two approaches to the analysis of fluid flow through the granular layer:

1. The flow in a granular layer is considered to be similar to the flow in a bundle of convoluted capillaries, in which the dispersion effects are attributed to various throughput and coordinating angles of spacing individual capillaries that form a common network of short capillary channels likened to the granular layer.
2. An approach to analyzing the granular layer with the presence of differently accessible volumes or dead zones, the presence of which at the time-varying concentration field causes dispersion effects measured relaxation coefficients of diffusion.

In this article, the capillary approach as the most studied one will be considered for the development of a mathematical model for the bioreactor with a close-packed layer of load. This approach is generally described in the reference¹¹. The flow analysis is based on the Kozeny–Carman equation:

$$\frac{\Delta p}{l} = k \frac{S_0^2 (1 - \varepsilon)^2}{\varepsilon^3} \mu \omega_{an} \quad (3)$$

where ω_{an} is the flow rate within the device, m/s

μ is the liquid viscosity, kg/m*s,

ε is the porosity layer,

k is the Kozeny constant,

S_0 is the specific layer surface determined by the expression, m²/m³:

$$S_0 = \frac{S_l}{\omega_{s.ph.}^2} = \frac{p h_l}{V_{s.ph.}} \quad (4)$$

where p is the “wetted” perimeter, m,

$V_{s.ph.}$ is the solid phase volume, m³,

h_l is the layer height, m.

For the polydisperse layer, S_0 will be determined by the following expression

$$S_0 = 6 \sum_i \frac{x_i}{d_i} \quad (5)$$

where x_i is a volume or mass ratio of the i -th fraction with the size d_i . These indicators are determined experimentally via the sieve method.

The Kozeny constant is determined according to¹⁰ based on the ratio:

$$k = \frac{2\varepsilon^3}{(1 - \varepsilon)[2\ln\{1/(1 - \varepsilon)\} - 3 + 4(1 - \varepsilon) - (1 - \varepsilon)^2]} \quad (6)$$

Furthermore, the study¹² indicates that the Kozeny–Carman equation can be also applied to the mixtures of differently sized particles, i. e. to the polydisperse layers by using a hydraulic radius therein instead of the diameter of particles in the monodisperse layers. The hydraulic radius is understood to mean the ratio of the cross-sectional area of the flow to its wetted perimeter:

$$r_h = \frac{F_{f.m.}}{p} = \frac{V_{por}}{p h_l} \quad (7)$$

The porosity of the polydisperse layer is defined as the ratio of pore volume to the granular layer volume:

$$\varepsilon = \frac{V_{por}}{V_l} \quad (8)$$

To calculate the flow rate within the pore space of a polydisperse layer, an equivalent pore diameter shall be determined using the following formula:

$$d_\varepsilon = \frac{4\varepsilon}{S_0(1 - \varepsilon)} \quad (9)$$

The average rate of the fluid flow in the pore channels of a granular layer is determined by the expression¹⁰:

$$\omega_{av} = k' d_\varepsilon^2 \Delta p / \mu l_0 \quad (10)$$

where k' is a numerical coefficient,

d_ε is the equivalent diameter of the pore channel, m.

The coefficient k' is determined as follows

$$k' = \frac{T^2}{16k} \quad (11)$$

where k is the Kozeny–Carman coefficient which is determined in the experiments as $k \cong 5.0$,

T is the pore channel tortuosity coefficient, which was defined in¹⁰ as:

$$T = \frac{l_0}{l} = \frac{1}{\cos 45^\circ} = \sqrt{2} = 1.41 \quad (12)$$

For the granular layer consisting of particles with different diameters, the equivalent diameter of the pore channel d_ε is defined by the following ratio:

$$d_\varepsilon = \frac{2}{3} \cdot \frac{\varepsilon \varphi d_{av}}{(1 - \varepsilon)} \quad (13)$$

where φ is the form factor which equals to 1.0 for spherical particles,

ε is the porosity of the medium;

d_{av} is the average grain diameter in the layer, which is defined as follows:

$$d_{av} = \sum_i \frac{x_i}{d_i} \quad (14)$$

where x_i is a volume or mass ratio of the i -th fraction with the size d_i .

According to the law of continuity, the average flow rate in a pore channel with the length $l = l_0$, where l_0 is the thickness of the porous layer, is $1/\varepsilon$ times higher than the device’s free section flow rate ω and equals to ω/ε . For the channel with the length of $> l_0$, the tortuosity coefficient $T = l/l_0$ was previously introduced. Then, taking into account this coefficient, the relation between the average fluid flow rate in the pore channel and its projection on the direction of the total flow motion is $\omega_{av} = \omega_{ap} T/\varepsilon$.

The equation for the flow rate in the pore channels used in the mathematical model:

$$\omega = \frac{\varepsilon^3 \varphi^2 d_{av}^2}{36\mu K_0 T^2 (1 - \varepsilon)^2} \cdot \frac{\Delta p}{l_0} = k \cdot \frac{\Delta p}{\mu l_0} \quad (15)$$

where k is the permeability coefficient or the permittivity, and

K_0 is the coefficient depending on the shape of the channel's cross section.

In the majority of cases, $K_0 = 2$ can be taken for the spherical particles¹³. If a particulate material is used as the catalyst, it is necessary to consider the kinetics of the chemical reactions occurring on the surface. To do this, one should evaluate the adsorption/desorption of the reactants at the surface of the particulate catalyst, know the particles slip velocity, and estimate the diffuse flow component. Fluctuations of such quantities as the specific surface of particles a and the porosity ε occur in the granular layer. On the one hand, these fluctuations are defined by the discreteness of the system consisting of individual grains, and on the other hand, by the macroscopic inhomogeneities of laying. The heterogeneity of the granular layer structure also causes the inhomogeneity in the distribution of fluid or gas flow rates penetrating the layer. These characteristics of the flow structure determine the internal hydrodynamics of the granular layer and the nature of the transport processes therein. A continuous change in the section and the direction of the pore channel between grains leads to sharp changes in the flow rate vector \vec{u} from point to point and causes, on the one hand, the displacement of neighboring filaments within the low-value range of the Reynolds number (Re) and, on the other hand, the occurrence of portions with a sharply lowered flow rate—dead zones. Averaging the vector \vec{u} over the sufficiently large representative volumes V leads to the introduction of the 'average local flow rate' concept. According to the literature, it is known¹³ that the flow rate in a wall boundary layer can vary by tens of percent from the rate in the reactor's central zone. Therefore, it is assumed in the models that in the large volumes the fluid moves through the granular layer in abreast. Furthermore, in the majority of processes involving the granular layer, the concentration of reactants in the flow, in the interstices between the grains, is unstable in both time and space. In the processes of adsorption (desorption) and at chemical reactions occurring on the surface of the catalyst grains, the sources of changes in the concentration of mixture components can be distributed with a varying intensity in the granular layer volume. Concentrations can also vary at the flow inlet into the granular layer and propagate along the device as a concentration wave. In these processes, the diffusion of mixture components plays an important role in both longitudinal and transverse directions within the device. The mathematical model described herein introduces the consideration of these phenomena.

The component concentration flow \vec{j}_c is determined not only through the transfer along with the bulk of the fluid at a rate \vec{u} , but also through the diffusion into adjacent regions:

$$\vec{j}_c = \vec{u}C - D\text{grad } C \quad (16)$$

where C is a local concentration, mol/L, and D is the diffusion coefficient of a given component within the flow. By compiling the material balance of a substance for the elementary volume, the following is obtained:

$$\frac{\partial C}{\partial \tau} = -\text{div}(\vec{u}C - D\text{grad } C) + q_c \quad (17)$$

For the incompressible fluid, $\text{div } \vec{u} = 0$, and

$$\frac{\partial C}{\partial \tau} = -\vec{u}\text{grad } C + \text{div}(D\text{grad } C) + q_c \quad (18)$$

In terms of devices with granular layer, the cylindrical type is the most convenient type of coordinates. In these coordinates, the above equation can be written as follows:

$$\varepsilon \frac{\partial c}{\partial \tau} + \omega_{(r)} \frac{\partial c}{\partial x} = \frac{\partial}{\partial x} \left[D_{l(r)} \frac{\partial c}{\partial x} \right] + \frac{1}{r} \cdot \frac{\partial}{\partial x} \left[r D_{r(r)} \frac{\partial c}{\partial r} \right] + q_c \quad (19)$$

where c is the concentration of a substance diffusing in the granular layer, mol/L or g/L;

$\omega_{(r)}$ is the fluid motion rate along the axis x related to the total cross section of the device, which is generally a function of the ordinate r , m/s;

τ is the time, s;

D_l and D_r are the diffusion coefficients according to the main coordinate axes x and r , respectively;

q_c is the intensity of the given substance release or absorption related to the unit of layer volume, mol/m³.

Based on the equation (19), as part of this study, the equations for biodiesel fuel, oil and alcohol were developed.

For biodiesel fuel:

$$\varepsilon \frac{\partial c_{bf}}{\partial \tau} + \omega_{(r)} \frac{\partial c_{bf}}{\partial x} = \frac{\partial}{\partial x} \left[D_{l(r)} \frac{\partial c_{bf}}{\partial x} \right] + \frac{1}{r} \cdot \frac{\partial}{\partial x} \left[r D_{r(r)} \frac{\partial c_{bf}}{\partial r} \right] + v \quad (20)$$

where:

c_{bf} is the concentration of biodiesel fuel;

v is the reaction rate of enzymatic catalysis determined by the equation (2).

The following equation is developed for oil:

$$\varepsilon \frac{\partial c_o}{\partial \tau} + \omega_{(r)} \frac{\partial c_o}{\partial x} = \frac{\partial}{\partial x} \left[D_{l(r)} \frac{\partial c_o}{\partial x} \right] + \frac{1}{r} \cdot \frac{\partial}{\partial x} \left[r D_{r(r)} \frac{\partial c_o}{\partial r} \right] - v \quad (21)$$

where:

c_o is the oil concentration.

The following equation is developed for alcohol:

$$\varepsilon \frac{\partial c_a}{\partial \tau} + \omega(r) \frac{\partial c_a}{\partial x} = \frac{\partial}{\partial x} \left[D_{1(r)} \frac{\partial c_a}{\partial x} \right] + \frac{1}{r} \cdot \frac{\partial}{\partial x} \left[r D_{r(r)} \frac{\partial c_a}{\partial r} \right] - v \quad (22)$$

where:

c_a is the alcohol concentration.

2.2 Determination of the Lipase Temperature Stability

The lipase temperature stability was determined using the methodology presented in¹⁴.

2.3 Yeast Cultivation Method

The *Yarrowia lipolytica* D6 recombinant yeast strain obtained from the Russian National Collection of Industrial Microorganisms was cultivated in 250 mL flasks filled with 125 mL working volume at 30 °C with constant stirring of 250 rpm. For culturing, the YNBD5%O5% medium was used, which comprises 5% of glucose and 5% of olive oil. The biomass culture in flasks was carried out by adding the 5×10^5 cells/mL titer of inoculum to the medium.

The inoculum was cultivated in 50 mL test tubes filled with 5 mL working volume at a constant temperature of 30 °C for 18 hours. The YPD medium was used to cultivate the inoculum.

2.4 Microalgae Cultivation Method

The study involves the culture of the *Chlorella vulgaris* GKV1 microalgae from the RDE "Kurchatov Institute" collection, which was cultured in the Basal medium¹⁵ with the following composition (g/L): KNO₃ – 1.25; KH₂PO₄ – 1.25; MgSO₄·7H₂O – 1.00; CaCl₂ – 0.0835; H₃BO₃ – 0.1142; FeSO₄·7H₂O – 0.0498; ZnSO₄·7H₂O – 0.0882; MnCl₂·4H₂O – 0.0144; MoO₃ – 0.0071; CuSO₄·5H₂O – 0.0157; Co(NO₃)₂·6H₂O – 0.0049; EDTA·2Na – 0.5. The growth medium was prepared using the filtered water. The initial pH value of the medium was 7.

The cultivation was carried out in the 250 mL, then in the 1,000 mL and finally in the 5,000 mL Erlenmeyer flasks under constant stirring by passing air bubbles (250 mL/min) at 24 ± 2 °C under constant (24/7) light intensity of 3,000 lux. Upon reaching a concentration of $20 \cdot 10^6$ cells/mL, the microalgae culture was separated by centrifugation, freeze dried and stored at -20 °C.

2.5 Obtaining the Fatty Acid Methyl Esters (FAME)

FAME were obtained through a direct methanolysis according to¹⁶.

2.6 GLC-analysis of FAME

A quality FAME analysis was performed using a gas chromatograph Bruker 430-GC in accordance with¹⁷.

2.7 Method of Preparing Granules for Loading

Granules for loading are made of polyacrylamide (PAA) with the yeast biomass immobilized thereon. The granules serve as a biocatalytic load into a close-packed layer bioreactor.

To prepare granules, the following reagents were used:

- PAA, a nonionic flocculant N-200 (manufactured by Fennopol, supplied by AkvaKhim);
- dodecyl alcohol, Purum grade (Khimmed, Russia).

The weighted amounts of biomass and polyacrylamide were placed in the 85 mL glass weighing bottles with lid, closed with lid and stirred until a homogeneous mixture. Then 0.11 g of the weighted resultant mixture was placed into a 15 mL plastic Kahn's tube, into which 0.7 mL of distilled water was pipetted. After forming the polyacrylamide gel with an immobilized biomass, 10 mL of dodecyl alcohol were added into the tube. The tubes were closed with a screwable lid and left for a day to form granules with immobilized biomass. After one day, the dodecyl alcohol was removed from the tubes using a pipette, and the resulting granules were dried in a fume hood for one hour.

3. Results

The calculations were performed for a reactor with 200 mL of loading capacity and inner diameter of 50 mm. The studies were conducted at 37 °C for each alcohol/oil variant.

Table 1 presents comprehensive data on the calculation results obtained by means of a mathematical model for the methanol with microalgae lipids reaction.

For the continuous flow bioreactor, the results on the degree of conversion for lipids and microalgae and methanol starting with the 1 : 4 oil to methanol ratio

turned out to be higher than 92%, while the maximum output of 94% can be achieved at the 1 : 6 and 2 : 7 ratios.

Table 2 presents data on the fatty acid composition of *C. Vulgaris* GKV1 microalgae obtained via the GC method.

The data presented in Table 3 shows that the maximum output of the biodiesel fuel during 48 hours in a continuous flow bioreactor can be achieved at the 1 : 4 to 1 : 5 ratios of microalgae lipids to methanol and constitutes 93%.

In general, it can be noted that for all variants of alcohols and oils, a close-packed layer bioreactor could provide an output of 90% or higher.

4. Discussion

As it can be seen from the results, the developed mathematical model shows a high agreement with the experimental data. This is primarily due to the fact that currently the process

Table 1. The conversion degree at using the microalgae lipids and methanol under different oil to methanol ratios

	Oil to methanol ratio								
	1 to 1	1 to 2	1 to 3	1 to 4	1 to 5	1 to 6	1 to 7	1 to 8	1 to 9
Time	Degree of conversion								
0	0	0	0	0	0	0	0	0	0
4	14	15	16	18	20	22	24	23	21
8	22	24	25	26	27	30	31	27	25
12	30	31	32	36	38	40	42	40	36
16	39	41	43	47	50	53	53	50	46
20	49	51	53	57	59	63	64	62	59
24	60	61	62	65	68	73	74	73	70
28	70	71	74	78	79	82	83	81	80
32	82	83	84	88	90	91	91	90	89
36	88	90	90	91	91	92	92	91	91
40	88	89	90	91	92	92	92	92	92
44	89	90	91	91	93	93	93	92	92
48	90	90	91	92	93	94	94	93	93

Table 2. The fatty acid composition of lipids of the *C. Vulgaris* GKV1 strain

No.:	Name	Time, min	Quantity, %
1	Palmitic (hexadecanoic) acid (16 : 0)	11.25	38.63
2	Palmitoleic acid (16 : 1)	11.53	1.69
3	(16 : 2)	12.30	6.11
4	Hexadecatrienoic acid (16 : 3)	12.48	4.99
5	Margaric-oleic acid (17 : 1)	13.87	1.97
6	Stearic (octadecanoic) acid (18 : 0)	15.44	2.07
7	Oleic acid (18 : 1)	15.80	8.13
8	Linoleic acid (18 : 2)	16.78	16.15
9	Nonadecanoic acid (19 : 0)	18.14	5.66
10	Arachidic (eicosanoic) acid (20 : 0)	23.08	1.91
11	Gadoleic acid (20 : 1)	23.26	3.83
12	Behenic (docosanoic) acid (22 : 0)	23.39	6.68
13	Cetoleic acid (22 : 1)	23.66	2.18
Total:			100

Table 3. The results of experiments on determining the optimum oil to alcohol ratio

	Lipids to methanol ratio								
	1 to 1	1 to 2	1 to 3	1 to 4	1 to 5	1 to 6	1 to 7	1 to 8	1 to 9
Time	Degree of conversion								
0	0	0	0	0	0	0	0	0	0
4	11	12	14	17	16	15	13	13	12
8	19	20	22	25	24	23	22	21	20
12	27	29	30	33	32	32	31	30	29
16	36	38	40	42	42	41	40	39	38
20	46	49	51	53	52	50	49	49	47
24	58	59	61	64	63	62	61	60	59
28	68	70	71	73	73	71	70	69	68
32	79	80	81	83	84	82	82	81	80
36	87	88	89	90	90	89	88	87	87
40	88	89	90	91	91	90	89	89	88
44	89	90	91	92	92	91	90	90	89
48	90	90	91	93	93	92	91	90	90

of enzyme catalysis of a transesterification reaction has been well studied, and there are its detailed mathematical descriptions⁶⁻⁹. Thus, the problem of the given process mathematical modeling is reduced to an adequate description of hydraulic processes within the bioreactor and the choice of one of the models describing the kinetics of the reaction. In case of the continuous flow bioreactor, the diffusion component in the description of hydraulic processes is critical, considering the fact that oil and alcohol are the immiscible liquids under normal conditions. Currently creating an adequate hydraulic model still remains a challenge for such a complex medium like the forcibly mixed alcohol/oil/esters/glycerin provided that they are constantly changing their concentrations. Changing the concentrations of given compounds leads to a permanent change in the rheological properties of the mixture, which further complicates the development of a mathematical model. At the same time, the approximated approaches similar to those proposed in this article can be applied to solve practical problems in case they provide sufficient accuracy. For example, these models can be used at the stage of manufacturing engineering or when designing new continuous flow bioreactors. They may also be useful when creating new types of catalyst loading for the existing bioreactors to predict potential changes in their operating characteristics.

It should be noted that the creation of continuous flow bioreactors requires developing a catalyst loading, which

in turn raises the problem of immobilizing cells (as in this article) or enzymes on various carriers. Currently no universal approaches established in this area have been developed. A separate carrier material shall be selected for each organism and each behavior medium condition⁴. A wide variety of possible carrier materials that are now available requires a tool to assess their applicability and effectiveness before starting the manufacture of a finished product. A mathematical modeling similar to that shown in the article can help in such situation by simulating the work of a bioreactor based on the data obtained in the laboratory.

5. Conclusion

The data obtained using a mathematical model correlate well with the experimental data, which enables the talks on its applicability in practice. Also based on the data obtained, it can be concluded that the continuous flow close-packed layer bioreactor is a carrier promising for industrial use, as it provides more than 90% of output after 48 hours of reaction.

6. Acknowledgement

This work was financially supported by the Ministry of Education and Science of the Russian Federation in the framework of the agreement on granting subsidies No.

14.607.21.0034. Unique identifier of the applied scientific research (project) RFMEFI60714X0034.

7. References

1. Fjerbaek L, Christensen KV, Norddahl B. A review of the current state of biodiesel production using enzymatic transesterification. *Biotechnology and Bioengineering*. 2009; 102:1298–315. DOI: 10.1002/bit.22256.
2. Yuzbasheva EY, Yuzbashev TV, Perkovskaya, NI, Mostova EB, Vybornaya TV, Sukhozhenko AV, Sineoky SP. Cell surface display of *Yarrowia lipolytica* lipase Lip2p using the cell wall protein YIPir1p, its characterization, and application as a whole-cell biocatalyst. *Applied Biochemistry and Biotechnology*. 2015; 175(8):3888–900. DOI: 10.1007/s12010-015-1557-7.
3. Pozhidaev VM, Gorin KV, Ulyanov YuV, Savin KA, Sergeeva YaE, Komova AV, Borgolov AV, Vasilov RG. Modern technologies for biodiesel fuel production. *Bulletin of Biotechnology and Physical and Chemical Biology*. 2015; 11(3):20–39.
4. Gotovtsev PM, Yuzbashev EYu, Gorin KV, Butylin VV, Badranova GU, Perkovskaya NI, Mostova EB, Namsaraev ZB, Rudneva NI, Komova AV, Vasilov RG, Sineokiy SP. Immobilization of microbial cells for the biotechnological production: Modern solutions and advanced technologies. *Applied Biochemistry and Microbiology*. 2015; 51(8):792–803.
5. Zhao X, Qi F, Yuan C, Du W, Liu D. Lipase-catalyzed process for biodiesel production: Enzyme immobilization, process simulation and optimization. *Renewable and Sustainable Energy Reviews*. 2015; 44:182–97. DOI: 10.1016/j.rser.2014.12.021.
6. Cheirsilp B, H-Kittikun A, Limkatanyu S. Impact of transesterification mechanisms on the kinetic modeling of biodiesel production by immobilized lipase. *Biochemical Engineering Journal*. 2008; 42(3):261–9. DOI: 10.1016/j.bej.2008.07.006.
7. Fedosov SN, Brask J, Pedersen AK, Nordblad M, Woodley JM, Xu X. Kinetic model of biodiesel production using immobilized lipase *Candida Antarctica* lipase B. *Journal of Molecular Catalysis B: Enzymatic*. 2013 Jan; 85–86:156–68. DOI: 10.1016/j.molcatb.2012.09.011.
8. Romero MD, Calvo L, Alba C, Daneshfar A. A kinetic study of isoamyl acetate synthesis by immobilized lipase-catalyzed acetylation in n-hexane. *Journal of Biotechnology*. 2007; 127:269–77. DOI: 10.1016/j.jbiotec.2006.07.009.
9. Haigh KF, Vladislavljević GT, Reynolds JC, Nagy Z, Saha B. Kinetics of the pre-treatment of used cooking oil using Novozyme 435 for biodiesel production. *Chemical Engineering Research and Design*. 2014; 92(4):713–19. DOI: 10.1016/j.cherd.2014.01.006.
10. Gromoglasov AA, Kopylov AS, Pil'shchikov AP. Water treatment: processes and devices. *Energoatomisdat Publication Company: Moscow*; 1990.
11. Happel J, Brenner G. *Hydrodynamics at low Reynolds numbers*. Mir Publication Company: Moscow; 1976.
12. Carman PC. *Flow of gases through porous media*. Academic Press: New York; 1956.
13. Aerov ME, Todes OM. *Hydraulic and thermal operational basics of devices with fixed and fluidized granular layer*. L.: Chemistry; 1968. p. 512.
14. Jackson MB. *Molecular and cellular biophysics*. M.: BINOM. Laboratory of Knowledge; 2012. p. 551.
15. Yeh KL, Chang JS. Effects of cultivation conditions and media composition. *Bioresource Technology*. 2012; 105:120–7. DOI: 10.1016/j.biortech.2011.11.103.
16. Liu J. Direct transesterification of fresh microalgal cells. *Bioresource Technology*. 2015; 176:284–7. DOI: 10.1016/j.biortech.2014.10.094.
17. Pozhidaev VM, Sergeyeva YaE, Gorin KV, Badranova GU, Gotovtsev PM, Borgolov AV, Vasilov RG. Determining a degree of the microbiological synthesis product conversion into biodiesel through gas chromatography. *Journal of Analytical Chemistry*. 2016; 71(6):653–9.